


BRAIN COMMUNICATIONS

Cohort study of electroencephalography markers of amyloid-tau-neurodegeneration pathology

Sean Tanabe,¹ Amber Bo,¹  Marissa White,¹ Margaret Parker,¹ Zahra Farahbakhsh,¹ Tyler Ballweg,¹ Cameron Casey,¹  Tobey Betthausen,² Henrik Zetterberg,^{3,4,5,6} Kaj Blennow,^{3,4} Brad Christian,⁷ Barbara B. Bendlin,² Sterling Johnson,² and Robert D. Sanders^{8,9}

Electroencephalography signatures of amyloid- β , tau and neurodegenerative pathologies would aid in screening for, tracking progression of, and critically, understanding the pathogenesis of dementia. We hypothesized that slowing of the alpha peak frequency, as a signature of hyperpolarization-activated cyclic nucleotide gated ‘pacemaker’ channel activity, would correlate with amyloid and tau pathology burden measured by amyloid (Pittsburgh Compound B) and tau (MK-6240) positron emission tomography or CSF biomarkers. We also hypothesized that EEG power would be associated with neurodegeneration (CSF neurofilament light and hippocampal volume). Wakeful high-density EEG data were collected from 53 subjects. Both amyloid- β and tau pathology were associated with slowing in the alpha peak frequency [Pittsburgh Compound B (+) vs. Pittsburgh Compound B (-) subjects, $P=0.039$ and MK-6240 (+) vs. MK-6240 (-) subjects, $P=0.019$]. Furthermore, slowing in the peak alpha frequency correlated with CSF A $\beta_{42/40}$ ratio ($r^2 = 0.270$; $P=0.003$), phosphoTau (pTau₁₈₁, $r^2 = 0.290$; $P=0.001$) and pTau₁₈₁/A β_{42} ($r^2 = 0.343$; $P<0.001$). Alpha peak frequency was not associated with neurodegeneration. Higher CSF neurofilament light was associated with lower total EEG power ($r^2 = 0.136$; $P=0.018$), theta power ($r^2 = 0.148$; $P=0.014$) and beta power ($r^2 = 0.216$; $P=0.002$); the latter was also associated with normalized hippocampal volume ($r^2 = 0.196$; $P=0.002$). Amyloid-tau and neurodegenerative pathologies are associated with distinct electrophysiological signatures that may be useful as mechanistic tools and diagnostic/treatment effect biomarkers in clinical trials.

- 1 Department of Anesthesiology, University of Wisconsin, Madison, WI, USA
- 2 Department of Medicine, Division of Geriatrics, University of Wisconsin, Madison, WI, USA
- 3 Department of Psychiatry and Neurochemistry, Institute of Neuroscience & Physiology, the Sahlgrenska Academy at the University of Gothenburg, Mölndal, Sweden
- 4 Clinical Neurochemistry Laboratory, Sahlgrenska University Hospital, Mölndal, Sweden
- 5 Department of Neurodegenerative Disease, UCL Institute of Neurology, London, UK
- 6 UK Dementia Research Institute at UCL, London, UK
- 7 Department of Medical Physics and Psychiatry, University of Wisconsin, Madison, WI, USA
- 8 Discipline of Anaesthetics, University of Sydney, Sydney, Australia
- 9 Royal Prince Alfred Hospital, Camperdown, NSW, Australia

Correspondence to: Robert Sanders, Department of Anaesthetics, Royal Prince Alfred Hospital, Building 89 Level 4/Lambie Dew Drive, Camperdown, NSW, 2050, Australia
E-mail: robert.sanders@sydney.edu.au

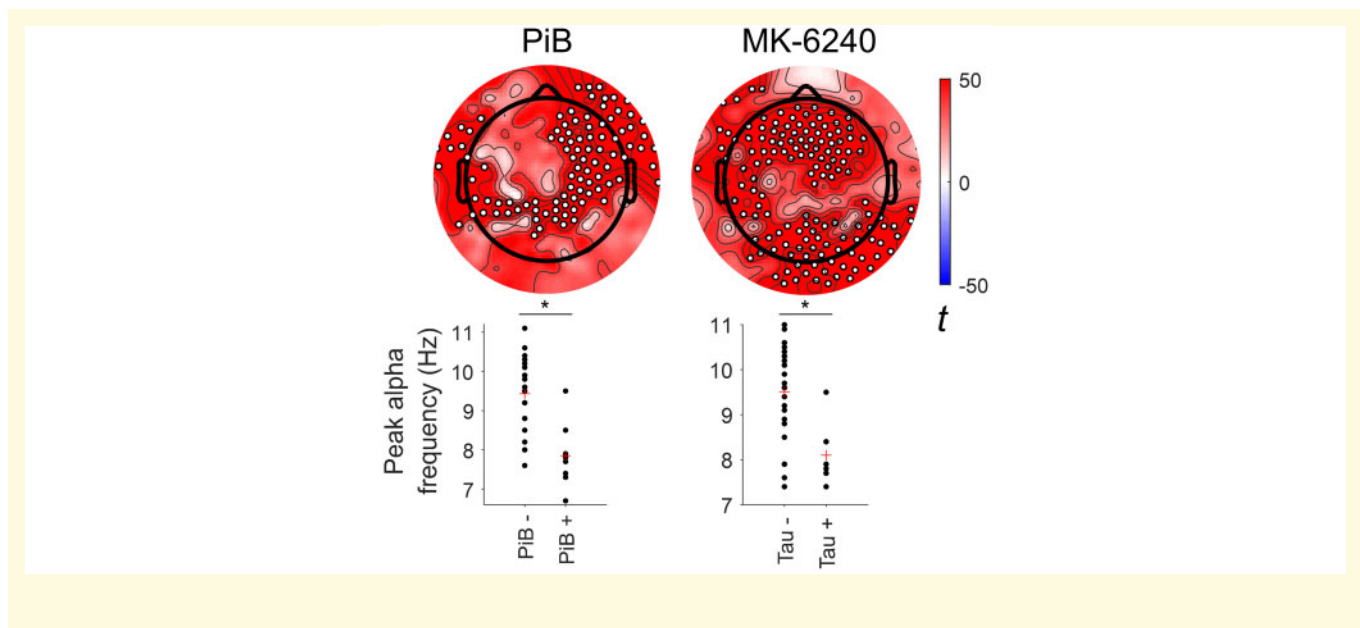
Received April 8, 2020. Revised May 23, 2020. Accepted June 1, 2020. Advance Access publication July 15, 2020

© The Author(s) (2020). Published by Oxford University Press on behalf of the Guarantors of Brain.

This is an Open Access article distributed under the terms of the Creative Commons Attribution Non-Commercial License (<http://creativecommons.org/licenses/by-nc/4.0/>), which permits non-commercial re-use, distribution, and reproduction in any medium, provided the original work is properly cited. For commercial re-use, please contact journals.permissions@oup.com

Keywords: amyloid; tau; neurodegeneration; EEG; alpha

Abbreviations: $A\beta$ = amyloid- β ; ATN = amyloid- β , tau and neurodegenerative; HCN = hyperpolarization-activated cyclic nucleotide gated; LZC = Lempel–Ziv complexity; NfL = neurofilament light; pTau = phosphoTau; TFCE = threshold free cluster enhancement.



Introduction

Dementia is associated with increased morbidity, and mortality, and significant impairments to quality of life (Jack and Holtzman, 2013). It costs billions of dollars in healthcare expenses annually yet there is a notable absence of treatments, whether preventative or therapeutic. Further understanding of the dementia pathophysiology is required to progress the field. This understanding should explain how synaptic and network changes contribute to cognitive decline and dementia. EEG can provide such information; herein, we sought to identify EEG correlates of preclinical dementia pathologies of amyloid, tau and neurodegeneration, the so called ATN pathologies (Jack *et al.*, 2018).

Our primary hypothesis was to test whether positron emission tomography (PET) for amyloid beta [$A\beta$ with Pittsburgh Compound B (PiB)] was associated with EEG slowing of the alpha peak in wakefulness. Slowing in this peak has previously been associated with dementia (Passero *et al.*, 1995) and mild cognitive impairment (Garces *et al.*, 2013). The cortical alpha rhythm is predominantly driven by pacemaker activity in infragranular cortical layer five (Karamah *et al.*, 2006). Early in the disease process, prior to neurodegeneration, amyloid disrupts layer five function, leading to slowing in supragranular layers (Lison *et al.*, 2014). $A\beta$ may achieve this through prolonging neuronal refractory periods (Kaczorowski *et al.*, 2011) mediated by impaired

hyperpolarization-activated cyclic nucleotide gated (HCN) ‘pacemaker’ channels that disappear in Alzheimer’s disease (Saito *et al.*, 2012). Loss of HCN channel function also augments $A\beta$ pathology (Saito *et al.*, 2012), perhaps through disruption of sleep (Lewis and Chetkovich, 2011). As computational studies show that loss of HCN channel function leads to slowing in the alpha frequency (Karamah *et al.*, 2006), we hypothesized that $A\beta$ pathology would lead to slowing in the peak alpha frequency, providing evidence to support the role of HCN channel function in Alzheimer’s disease pathogenesis. We also hypothesized that these changes would occur independent of changes in neurodegeneration (Lison *et al.*, 2014) but may be associated with tau pathology given the potential amyloid-tau disease continuum.

Our secondary endpoints focused on identifying dissociable EEG power correlates of ATN pathologies using EEG, PET, MRI and CSF data. For example, we specifically hypothesized that, while amyloid and tau pathologies may be associated with slowing in the alpha peak frequency, neurodegenerative pathologies would not be (as we lacked rationale for HCN channel disruption). Recent studies, published during the collection of our data, have proposed different markers of amyloid or neurodegenerative pathologies. Nakamura *et al.* (2018) suggested that increased normalized alpha power, identified on magnetoencephalography was the electrophysiological signature of amyloid pathology. This required complex source reconstruction (with various methodological assumptions) of

the signal, and given the expense and rarity of magnetoencephalography, this could not serve as a screening tool. Gaubert *et al.* (2019) uncovered complex relationships of EEG changes with amyloid and neurodegenerative pathologies. Their main findings were increases in power in higher frequencies with accumulating pathology, until later stages, where high frequency power decreased (Gaubert *et al.*, 2019). The inconsistent findings across these studies, highlight the need for more EEG studies. Ideally, these studies should be extended to include markers of brain tau pathology, using tracers such as [18F]MK-6240 (Betthausen *et al.*, 2019, 2020). We embarked on similar analyses in EEG in sensor space, avoiding the complexities of source reconstruction, to ascertain whether similar effects on alpha power would be observed in the EEG in our dataset.

We hypothesized that total power in the EEG would correlate with neurodegeneration based on prior findings suggesting EEG power was related to grey matter volume (Ni Mhuirheartaigh *et al.*, 2013). This is plausible given that a smaller mass of cortical tissue, with reduced synaptic connections, would be anticipated to generate fewer excitatory post-synaptic potentials and hence less EEG power. As a further exploratory analysis, we investigated whether Lempel–Ziv complexity (LZC) (Lempel and Ziv, 1976), a measure of information in the EEG, would change with ATN pathology (Jack *et al.*, 2018). We consider that this may be a useful marker of synaptic degeneration, where synaptic loss would decrease the repertoire of different firing states, reducing the complexity of EEG patterns.

Materials and methods

Participants, 18 years of age and older, were recruited from two parent studies, the Wisconsin Registry for Alzheimer's Prevention and the Alzheimer's Disease Research Center, where brain imaging (PET, MRI) data have been collected. The study was approved by the University of Wisconsin-Madison Institutional Review Board 2017-0821 and all participants provided informed consent. Our study was powered to show a 2 Hz difference in the peak alpha frequency between PiB(+) and PiB(-) groups ($\beta = 0.8$, $P < 0.05$) assuming a standard deviation of 2 Hz and a 20% PiB(+) rate in the cohort (Johnson *et al.*, 2014). This required 50 subjects. We recruited an additional 5% to account for missing data. We considered that only strong biological relationships would be of interest and that convergence of CSF and imaging findings would be required to give confidence in the results. When data were available from our surgical cohort [where we had data on preoperative plasma neurofilament light (NfL), EEG and MRI data] we also validated our findings in that cohort (Casey *et al.*, 2020) (see Supplementary Fig. 1 for STROBE diagram). The surgical cohort data are from preoperative assessments of patients

presenting for major elective surgery including EEG and blood collection reported in Casey *et al.* (2020). There are no patients with dementia and nine patients with mild cognitive impairment in that cohort.

EEG recording and preprocessing

Fifteen minutes of resting state EEG data with eyes closed were collected using 256 channel high-density EEG (Electrical Geodesics, Inc., Eugene, OR, USA) at sampling frequency of 250 Hz. Recordings were made in the sitting position. Subjects were told to close their eyes and relax, but not fall asleep, during the recordings. The EEG data were filtered (0.1–50 Hz) using a Hamming windowed sinc finite impulse response (FIR) filter. Artefacts were removed by visual inspection of channels and data segments. Artefacts of eye and muscle movements were removed by independent component analysis in EEGLAB. The removed channels were interpolated, and all the data were average-referenced.

EEG analysis

Alpha peak detection

The time series data were estimated for power spectral density by Welch's method. We defined the alpha peak frequency, using power spectrum bounded by 6–12 Hz, as the local maxima frequency with the highest prominence*width (at the half-prominence). We excluded subjects without an alpha peak by visually inspecting channel Fz power spectrum.

Average spectral power

The estimated power spectral density was averaged into band power; delta (0.5–4 Hz), theta (4–7 Hz), alpha (7–11 Hz), beta (11–28 Hz), gamma (28–40 Hz) and log10 transformed to normalize the distribution.

Lempel–Ziv complexity

In order to quantify the information in the EEG, we calculated LZC (Lempel and Ziv, 1976), the number of unique sub-string within a time series, to estimate the signal complexity related to dementia pathologies. Based on prior data in subjects with dementia (Fernandez *et al.*, 2010), we hypothesized that accumulation of dementia pathologies would be associated with reduced LZC. LZC is calculated on a binarized signal, which is transformed by coarse-grained data time series by binarizing above (1) or below (0) the median amplitude. Within the binarized signal, the LZC is the counted sum of sub-string, where the sub-strings are determined by iterating and counting unique sequences which has not been encountered in the signal sequence prior to it.

In the LZC analysis, we calculated and averaged LZC of 10 s segments across the data. We controlled for the

changes in power spectrum, by dividing LZC by phase shuffled LZC (Schartner *et al.*, 2015). The phase shuffled LZC is calculated by randomly phase shuffling the actual signal before applying LZC. We averaged 100 such randomly phase shuffled LZC before normalizing LZC.

Cerebrospinal fluid collection

The CSF collection was performed via lumbar puncture in the morning after a 12-h overnight fast, aliquoted in sterile polypropylene collection tubes, and stored in a -80°C freezer (Bendlin *et al.*, 2012). A centre-wide standard pre-analytical protocol was used to collect ~ 22 ml of CSF that was subsequently gently mixed to remove collection gradients, partitioned into 0.5-ml aliquots in 1.0-ml polypropylene tubes and stored at -80°C . Assayed analytes include total tau, phosphoTau (pTau₁₈₁), amyloid β_{1-42} (A β_{42}), amyloid β_{1-40} (A β_{40}) and NfL protein. CSF T-Tau, P-Tau₁₈₁ and A β_{42} were analysed by utilizing the INNO-BIA AkzBio3 kit (Innogenetics) using xMAP technology as previously described (Olsson *et al.*, 2005). CSF NfL was analysed using the sandwich ELISA method (Rosengren *et al.*, 1996). As previously reported, intra-assay coefficients of variation were below 10% for all analytes (Bendlin *et al.*, 2012). The time interval between CSF/PET and EEG was 10.3 months (standard deviation = 10.9 months).

PET imaging analysis

Amyloid- β imaging was conducted with [C-11] Pittsburgh Compound-B (PiB) PET using a dynamic 70-min protocol (Johnson *et al.*, 2014). Amyloid positive scans were defined qualitatively using established criteria (Johnson *et al.*, 2014). Tau PET imaging was conducted using [F-18]MK6240 from ~ 70 - to 110-min post-injection (Betthausen *et al.*, 2019, 2020). Tau-positive PET scans were defined by setting the MK-6240 SUVR positivity threshold at 2 standard deviation above the mean of the PiB(-) group in the entorhinal cortex (entorhinal MK-6240 SUVR > 1.27) as in Betthausen *et al.* (2020).

MRI protocol

Imaging included an inversion recovery-prepared T1-weighted 3D volume structural scan. The T1-weighted 3D volume was segmented into tissue classes (CSF, grey matter and white matter) using the segmentation tool in SPM12 (www.fil.ion.ucl.ac.uk/spm). CSF-to-brain volume ratio was calculated as the tissue volume ratio of CSF/(grey matter + white matter). Hippocampal volume was calculated using FSL-FIRST, a model-based segmentation/registration tool, and corrected for intracranial volume calculated in SPM12 as per recent methods paper (Keihaninejad *et al.*, 2010; Allison *et al.*, 2019).

Cognitive data

Boston Naming test, Category Fluency—Animals, Mini-Mental State Exam, Letter Fluency, Rey Auditory Verbal Learning Test, Trail Making Test A and B were all collected as part of this study. As a secondary analysis, EEG correlates of these cognitive data were also sought.

Statistical analysis

For topological analysis, we performed cluster-wise correlations and two-sided contrasts by statistical non-parametric mapping with threshold free cluster enhancement (TFCE). Alpha peak frequency or power changes were detected in each individual electrode and then a *t*-test or Spearman correlation was performed at each electrode with TFCE correction across electrodes. Only results that survived multiple comparison correction with TFCE across electrodes were considered statistically significant. However, in order to present raw data, we show the peak channel effect and report univariate *P*-values for that in the text (labelled as univariate *P*-values). Linear regression was conducted in R.

Data availability

Data are available upon reasonable request.

Results

Four subjects were excluded due to poor quality EEG recordings. Forty-nine subjects were included in the final analysis. The mean age was 70 years (standard deviation = 6.46 years), with 27 females and 22 males, the mean years of education was 16 years (standard deviation = 2.27), and the dataset include 5 subjects with mild cognitive impairment and 4 subjects with dementia. Forty-one had CSF, 45 had PiB PET scans and 44 had MK6240 PET scans.

Primary outcome

Alpha peaks could not be detected in 10 subjects. The 10 subjects who were excluded included 1 patient with mild cognitive impairment and 9 cognitively normal individuals but no subjects with dementia. After correcting for multiple corrections across electrodes, slowing in the peak alpha frequency was significantly associated with both PiB and MK6240 PET (Fig. 1). We additionally report the univariate results for the peak channel for illustration. Slowing in the alpha peak frequency occurred in amyloid positive [channel 221 Mann-Whitney U-test univariate $P=0.039$, AUROC 0.90, 95% confidence interval 0.78–1.02, $P=0.001$] and tau-positive individuals (channel 148 Mann-Whitney U-test univariate $P=0.019$, AUROC 0.86, 95% confidence interval 0.73–0.98, $P=0.003$). Next, we tested whether these results were robust to confounding by adjusting for age, sex, diagnosis and the time interval from PET scanning to EEG recording. In these analyses,

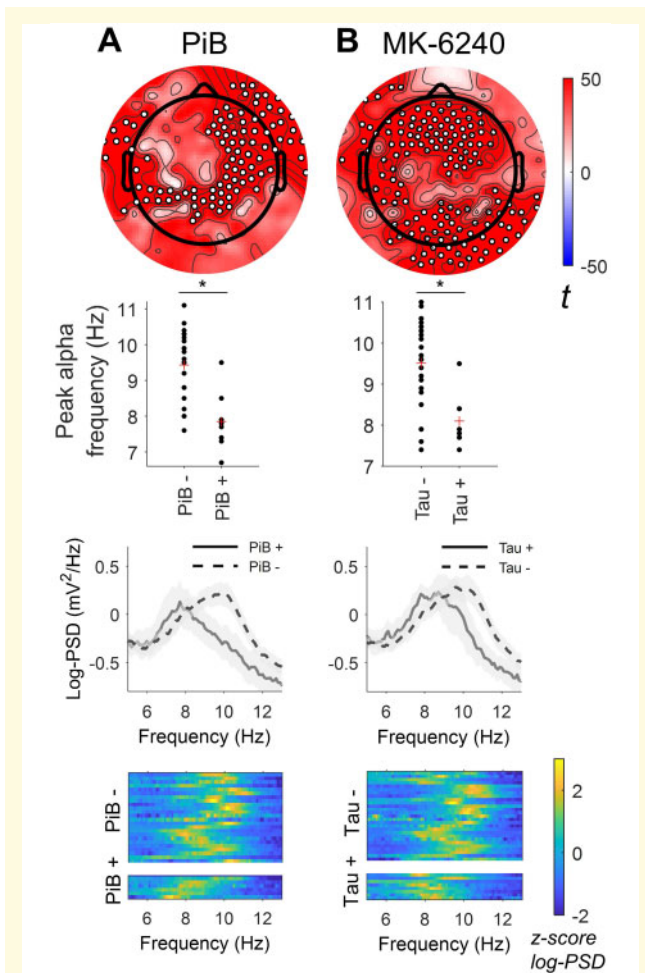


Figure 1 Pathological correlates of alpha peak frequency.

Top row: Correlations of PET PiB (A, $n = 30$) and MK-6240 (B, $n = 35$) with alpha peak frequency. All data are TFCE corrected $P < 0.05$ (white dots show statistically significant electrodes). Second row: An example electrode for the peak effect [channel 221 (a), channel 148 (b)]. Third row: The mean power spectrum in the alpha range for PET scans classified as positive or negative. Fourth row: Sorted z-score power spectrum by ranked values split on PET positive or negative for the alpha peak frequency.

using data from the electrode with the peak effect, PET scanning results remained significant (Table 1). *Post hoc*, we additionally tested whether the results remained significant after inclusion of diagnosis of either tau- or amyloid-positivity as a covariate in linear regression. In this sensitivity analysis, the results were unchanged.

After correcting for multiple corrections across electrodes, slowing in the peak alpha frequency correlated with CSF $A\beta_{42/40}$ (channel 2 $r^2 = 0.270$, univariate $P = 0.003$), pTau₁₈₁/ $A\beta_{42}$ (channel 129 $r^2 = 0.343$, univariate $P < 0.001$) and pTau₁₈₁ (channel 5 $r^2 = 0.290$; univariate $P = 0.001$) but not NfL (Fig. 2). We similarly confirmed that hippocampal volume did not correlate with alpha peak frequency in that subgroup (data not shown). Linear regression including age, sex, diagnosis

and the time interval between CSF sampling and the EEG as covariates did not alter these findings (Table 1).

Secondary outcome: EEG power as a signature of neurodegeneration

Consistent with our hypothesis, CSF NfL correlated with total EEG power (channel 120 $r^2 = 0.136$; univariate $P = 0.018$, Fig. 3). In different EEG power bands, the correlations were evident in theta power (channel 142 $r^2 = 0.148$; univariate $P = 0.014$) and beta power (channel 104 $r^2 = 0.216$; univariate $P = 0.002$, Fig. 3). The association of NfL and theta power survived adjustment for age, sex, diagnosis and the time interval between the test and the EEG (Table 1). Beta power narrowly missed significance (univariate $P = 0.061$).

In order to verify that these power changes were associated with neurodegeneration, we next tested for a correlation between total, theta and beta power with hippocampal volume after normalization for intracranial volume. Beta power, but not total or theta power, was associated with hippocampal volume (channel 25 beta power $r^2 = 0.196$; univariate $P = 0.002$, Fig. 3C). In our separate surgical cohort, we confirmed similar findings that both plasma NfL ($n = 48$) or hippocampal volume ($n = 30$) correlated with preoperative EEG total power (Supplementary Fig. 2).

Secondary outcome: EEG power as a signature of amyloid pathology

We next conducted exploratory analyses for alternative EEG signatures of amyloid and tau pathology across total power and the individual power bands. Given associations with total power with NfL, we also normalized each band by total power to identify if the changes were specific to that band. $A\beta$ pathology markers, PiB (Mann-Whitney U-test beta power univariate $P = 0.004$, normalized beta power univariate $P = 0.001$, Fig. 4A), and CSF $A\beta_{42/40}$ (normalized beta power $r^2 = 0.198$; univariate $P = 0.004$, Fig. 4B) correlated with beta power, but not other power bands. These results survived adjustment for age, sex, diagnosis and the time interval between the test and the EEG (Table 1). No other significant correlations were identified.

Secondary outcome: EEG signature of tau pathology

We did not identify alternate EEG signatures of CSF or PET tau pathology markers that survived multiple comparison correction across electrodes (data not shown).

Table 1 Linear regression with sex, mild cognitive impairment/dementia diagnosis, age at PET, CSF or MRI collection, and time between PET, CSF or MRI collection and EEG

| Dependent | Independent | Channel | n | T | P |
|---------------------------|---------------------------------|---------|----|-------|--------|
| Peak alpha frequency (Hz) | PiB | 221 | 30 | −3.85 | <0.001 |
| Peak alpha frequency (Hz) | MK-6240 | 148 | 35 | −2.53 | 0.017 |
| Peak alpha frequency (Hz) | pTau: Ab42 | 129 | 32 | −5.22 | <0.001 |
| Peak alpha frequency (Hz) | Ab42: Ab40 | 2 | 31 | 4.21 | <0.001 |
| Peak alpha frequency (Hz) | pTau | 5 | 32 | −3.31 | 0.003 |
| Peak alpha frequency (Hz) | NFL | 9 | 32 | −0.26 | 0.795 |
| Total power | NFL | 120 | 41 | −1.59 | 0.120 |
| Delta | NFL | 138 | 41 | −2.60 | 0.014 |
| Theta | NFL | 142 | 41 | −2.93 | 0.006 |
| Alpha | NFL | 122 | 41 | −1.60 | 0.118 |
| Beta | NFL | 104 | 41 | −1.93 | 0.061 |
| Gamma | NFL | 144 | 41 | −2.85 | 0.007 |
| Beta | Hippocampal/intracranial volume | 25 | 49 | 1.83 | 0.073 |
| Beta | PiB | 75 | 39 | −3.15 | 0.003 |
| Normalized beta | PiB | 52 | 39 | −3.93 | <0.001 |
| Beta | Ab42: Ab40 | 186 | 40 | 2.48 | 0.018 |
| Normalized beta | Ab42: Ab40 | 144 | 40 | 3.64 | <0.001 |

Linear regression on the peak effect channel.

Secondary outcome: pathology correlations with LZC

Both $A\beta$ and tau pathologies (but not neurodegeneration) were associated with reductions in LZC of the EEG that survived multiple comparisons; however, these effects disappeared when normalizing to a phase-shuffled distribution though individual channels showed the effect (unadjusted for multiple comparisons; [Supplementary Fig. 3](#)).

Secondary outcome: EEG correlations with cognitive data

Our cohort is largely cognitively unimpaired but, as exploratory analyses, we correlated the EEG alpha peak frequency or EEG power bands with cognitive data (Boston Naming test, Category Fluency—Animals, Mini-Mental State Exam, Letter Fluency, Rey Auditory Verbal Learning Test, Trail Making Test A and B) and found no significant associations between any of the EEG variables (data not shown).

Discussion

Our data show that EEG changes are associated with ATN pathologies ([Jack et al., 2018](#)). Our primary outcome, the association of amyloid positivity (PET and CSF) with slowing in the peak alpha frequency supports our hypothesis. Furthermore, the similar associations with tau pathology markers (CSF and PET) suggest that, as $A\beta$ and tau pathologies accumulate, so does slowing in the EEG. These findings are consistent with accumulating data suggesting HCN channel dysfunction in Alzheimer's disease (AD) ([Saito et al., 2012](#)). Understanding the

synaptic and network changes that precede cognitive and memory impairment in dementia is critical to the development of therapies that will improve quality of life and prolong an individual's independence. Our data suggest that further investigation of HCN channel function is warranted particularly as impaired function of these channels may also augment $A\beta$ pathology ([Saito et al., 2012](#)) and may explain the link between slow wave sleep disruption and impaired $A\beta$ clearance ([Rasmussen et al., 2018](#)).

Beyond changes in the peak alpha frequency, we did not identify further EEG signatures of tau pathology, as determined by CSF or PET. However, $A\beta$ pathology correlated with normalized beta power overlying temporal regions using both PET and CSF data. Importantly, our findings differ from the recent report by [Nakamura et al. \(2018\)](#) who showed, using magnetoencephalography in source space, that increased alpha power was a signature of $A\beta$. Whether this discordance represents real differences between the two cohorts (e.g. ethnically different) or technical differences with processing the EEG/magnetoencephalography data are unclear. However, we emphasize that we verified our results with two different measures of pathology (CSF and PET). Overall our findings are more consistent with the findings of [Gaubert et al. \(2019\)](#) who showed correlations with EEG slowing, however, neither of these other studies reported on peak alpha frequency ([Nakamura et al., 2018](#); [Gaubert et al., 2019](#)).

Loss of beta power was correlated with CSF and imaging markers of neurodegeneration and may reflect loss, or impaired function of interneurons that generate this rhythm ([Porjesz et al., 2002](#); [Palop and Mucke, 2016](#)). If so, this loss of beta power may identify individuals in whom augmenting GABAergic signalling may improve cognitive function ([Palop and Mucke, 2016](#)).

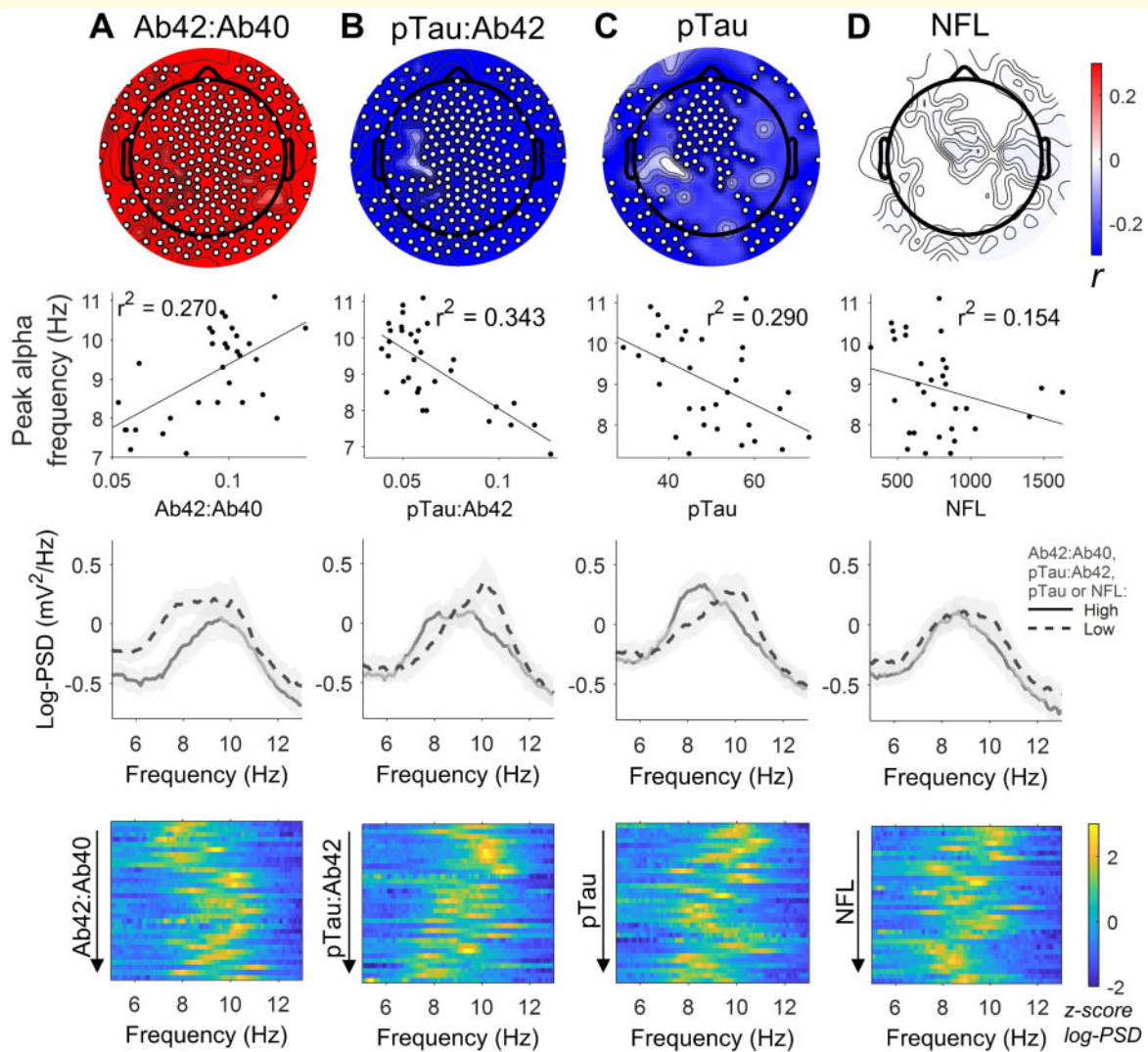


Figure 2 Pathological correlates of alpha peak frequency. Top row: Correlations of alpha peak frequency with CSF Ab42:40 (A, $n = 31$), pTau/Ab42 (B, $n = 32$), pTau (C, $n = 32$) and NFL (E, $n = 32$) are also shown. All data are TFCE corrected $P < 0.05$ (white dots show statistically significant electrodes). Second row: An example electrode, peak effect [channel 2 (A), 129 (B), 5 (C), 9 (D)], is also shown for the correlation with alpha peak frequency. Third row: The mean power spectrum in the alpha range after median split in the CSF biomarker. Fourth row: Sorted z-score power spectrum by ranked values in CSF biomarkers for the alpha peak frequency.

Additionally, we validated that neurodegeneration was associated with reduced EEG power with data from our surgical cohort (Casey *et al.*, 2020) (focusing on total power, in line with our original hypothesis). An association between grey matter volume and EEG power has been proposed previously in a younger population (Ni Mhuircheartaigh *et al.*, 2013). The results of the current study, albeit in a more elderly population, are consistent with these prior findings. The association of reduced EEG power and neurodegeneration is particularly intriguing given that it is well established that increases in theta and delta power (EEG slowing) occur with dementia (Babiloni *et al.*, 2018; Gaubert *et al.*, 2019). Normalization for these neurodegenerative changes would be expected to exaggerate this effect, hence prior studies

may have underestimated the changes in EEG slowing that occur at a synaptic level.

Changes in information, reflected by LZC, were also noted with A β and tau pathology, consistent with early synaptic loss in AD (Palop and Mucke, 2016). However, the effect on LZC did not survive correction for multiple comparisons after we shuffled the phase distribution (though single electrodes still showed the effect). This suggests that A β and tau pathologies may contribute to the fade in the information in cortex that occurs with progression to dementia; however, further data are needed to robustly confirm this hypothesis. Future work should also evaluate links between reduced LZC and synaptic loss with new PET tracers that target synaptic density (Chen *et al.*, 2018).

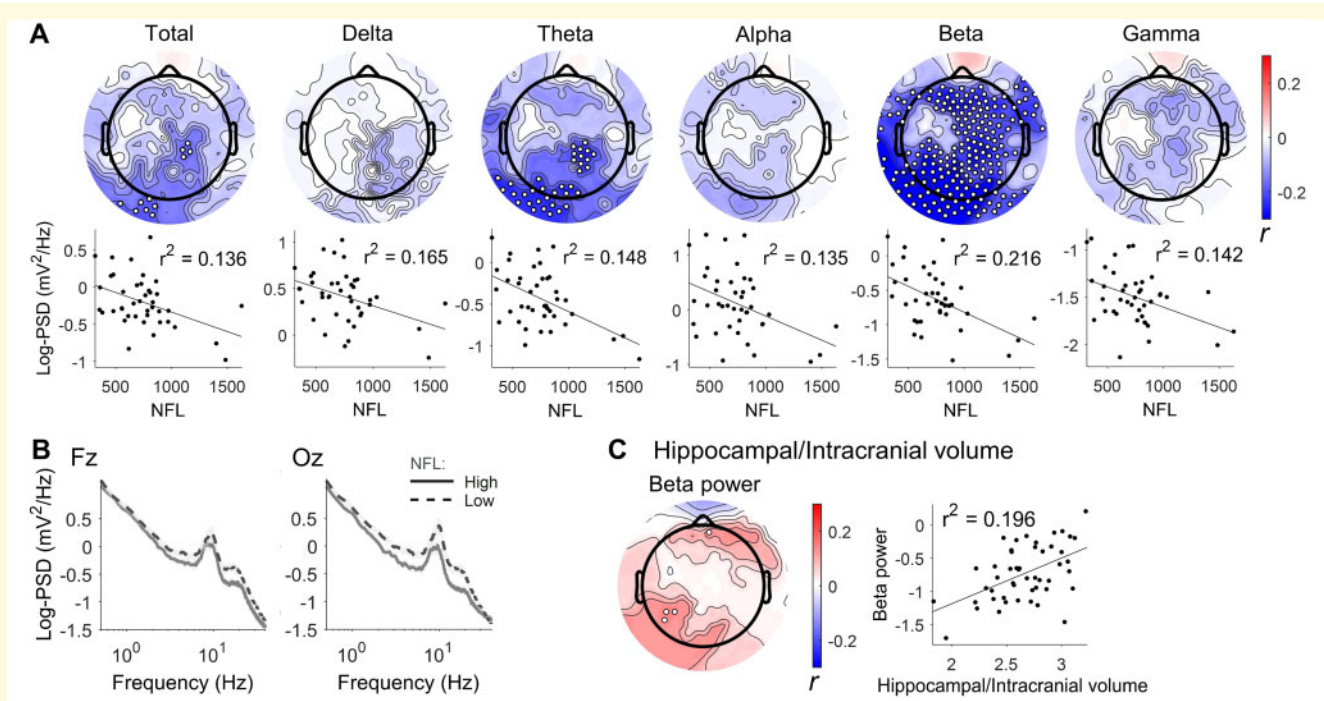


Figure 3 EEG power correlates of NFL. (A) $n = 41$, SnPM correlation, corrected TFCE $P < 0.05$ (white dots show statistically significant electrodes). (B) EEG power by median split on CSF NFL values. (C) Correlations in beta power with hippocampal volume normalized by intracranial volume. Peak effect electrodes are plotted [(A) total power channel 120, delta power channel 138, theta power channel 142, alpha power channel 122, beta power channel 104, gamma power channel 144; (C) beta power channel 25].

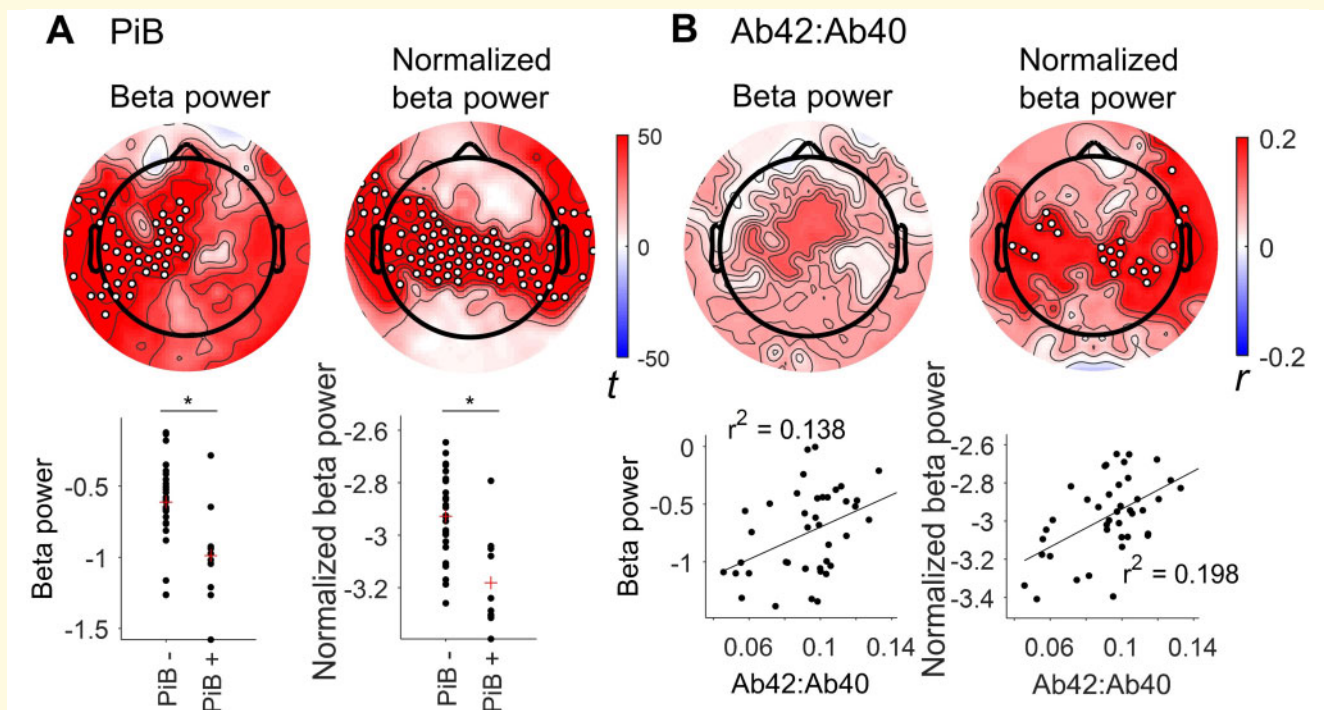


Figure 4 Beta power and normalized beta power correlates of PET PiB (A, $n = 39$) and CSF amyloid (B, $n = 40$). SnPM correlation, corrected TFCE $P < 0.05$ (white dots show statistically significant electrodes). Example channels are plotted for the peak effects, (A) channel 75 and channel 52, (B) channel 186 and channel 144.

Our cohort was relatively small and designed to only identify strong, biologically plausible relationships based on *a priori* determined hypotheses. We also adjusted for multiple comparisons across electrodes and conducted linear regression to adjust for potential confounders that included age, sex, diagnosis, time between the biomarker and the EEG collection. It is important to note that these findings need validation in future cohorts, and we cannot establish causality in our observational study design which may be vulnerable to unmeasured confounding. A strength of our analysis was the focus on sensor, not source, EEG metrics which are straightforward analytically. Nonetheless, we encountered some technical difficulties, similar to prior studies, in detecting the alpha peak in 10 individuals. Our data show that it is possible to detect EEG abnormalities that arise as a result of ATN pathologies, supportive of potentially using EEG as a non-invasive screening tool for AD pathology. This could improve the accessibility of biomarker screening, as well as providing mechanistic clues regarding the synaptic dysfunction that accompanies dementia disease progression. Next, it will be important to track EEG markers, within individuals, over time to identify if this may be a useful strategy for monitoring ATN pathology progression in the elderly and as potential biomarkers for therapies targeting interneuron dysfunction (Palop and Mucke, 2016) or HCN channel activity (Saito *et al.*, 2012).

Supplementary material

Supplementary material is available at *Brain Communications* online.

Acknowledgements

Thanks to Drs Brady Riedner and Giulio Tononi for advice and loan of equipment.

Funding

This work was supported by National Institute of Health (P30AG062715). R.D.S. is additionally supported by National Institute of Health (1R01AG063849-01 and 1K23AG055700-01A1). H.Z. is a Wallenberg Scholar supported by grants from the Swedish Research Council (#2018-02532), the European Research Council (#681712), Swedish State Support for Clinical Research (#ALFGBG-720931) and the UK Dementia Research Institute at UCL. K.B. is supported by the Swedish Research Council (#2017-00915), the Alzheimer Drug Discovery Foundation (ADDF), USA (#RDAPB-201809-2016615), the Swedish Alzheimer Foundation (#AF-742881), Hjärnfonden, Sweden (#FO2017-0243), the Swedish state under the agreement between the Swedish government and the County Councils, the ALF-agreement (#ALFGBG-715986) and European Union

Joint Program for Neurodegenerative Disorders (JPND2019-466-236).

Competing interests

H.Z. has served at scientific advisory boards for Denali, Roche Diagnostics, Wave, Samumed and CogRx, has given lectures in symposia sponsored by Fujirebio, Alzecure and Biogen, and is a co-founder of Brain Biomarker Solutions in Gothenburg AB, a GU Ventures-based platform company at the University of Gothenburg. K.B. has served as a consultant or at advisory boards for Abcam, Axon, Biogen, Lilly, MagQu, Novartis and Roche Diagnostics, and is a co-founder of Brain Biomarker Solutions in Gothenburg AB, a GU Venture-based platform company.

References

- Allison SL, Kosciak RL, Cary RP, Jonaitis EM, Rowley HA, Chin NA, et al. Comparison of different MRI-based morphometric estimates for defining neurodegeneration across the Alzheimer's disease continuum. *NeuroImage Clin* 2019; 23: 101895.
- Babiloni C, Del Percio C, Lizio R, Noce G, Lopez S, Soricelli A, et al. Abnormalities of resting state cortical EEG rhythms in subjects with mild cognitive impairment due to Alzheimer's and Lewy body diseases. *J Alzheimer Dis* 2018; 62: 247–68.
- Bendlin BB, Carlsson CM, Johnson SC, Zetterberg H, Blennow K, Willette AA, et al. CSF T-Tau/Abeta42 predicts white matter microstructure in healthy adults at risk for Alzheimer's disease. *PLoS One* 2012; 7: e37720.
- Bethausen TJ, Cody KA, Zammit MD, Murali D, Converse AK, Barnhart TE, et al. In vivo characterization and quantification of neurofibrillary tau PET radioligand [(18)F]MK-6240 in humans from Alzheimer's disease dementia to young controls. *J Nucl Med* 2019; 60: 93–9.
- Bethausen TJ, Kosciak RL, Jonaitis EM, Allison SL, Cody KA, Erickson CM, et al. Amyloid and tau imaging biomarkers explain cognitive decline from late middle-age. *Brain* 2020; 143: 320–35.
- Casey CP, Lindroth H, Mohanty R, Farahbakhsh Z, Ballweg T, Twadell S, et al. Postoperative delirium is associated with increased plasma neurofilament light. *Brain* 2020; 143: 47–54.
- Chen MK, Mecca AP, Naganawa M, Finnema SJ, Toyonaga T, Lin SF, et al. Assessing synaptic density in Alzheimer disease with synaptic vesicle glycoprotein 2A positron emission tomographic imaging. *JAMA Neurol* 2018; 75: 1215–24.
- Fernandez A, Hornero R, Gomez C, Turrero A, Gil-Gregorio P, Matias-Santos J, et al. Complexity analysis of spontaneous brain activity in Alzheimer disease and mild cognitive impairment: an MEG study. *Alzheimer Dis Assoc Disord* 2010; 24: 182–9.
- Garces P, Vicente R, Wibrall M, Pineda-Pardo JA, Lopez ME, Aurteneixe S, et al. Brain-wide slowing of spontaneous alpha rhythms in mild cognitive impairment. *Front Aging Neurosci* 2013; 5: 100.
- Gaubert S, Raimondo F, Houot M, Corsi MC, Naccache L, Diego Sitt J et al.; Alzheimer's Disease Neuroimaging Initiative. EEG evidence of compensatory mechanisms in preclinical Alzheimer's disease. *Brain* 2019; 142: 2096–112.
- Jack CR, Jr., Bennett DA, Blennow K, Carrillo MC, Dunn B, Haeblerlein SB, et al. NIA-AA research framework: toward a biological definition of Alzheimer's disease. *Alzheimer's Dement* 2018; 14: 535–62.
- Jack CR, Jr., Holtzman DM. Biomarker modeling of Alzheimer's disease. *Neuron* 2013; 80: 1347–58.

- Johnson SC, Christian BT, Okonkwo OC, Oh JM, Harding S, Xu G, et al. Amyloid burden and neural function in people at risk for Alzheimer's disease. *Neurobiol Aging* 2014; 35: 576–84.
- Kaczorowski CC, Sametsky E, Shah S, Vassar R, Disterhoft JF. Mechanisms underlying basal and learning-related intrinsic excitability in a mouse model of Alzheimer's disease. *Neurobiol Aging* 2011; 32: 1452–65.
- Karamah FN, Dahleh MA, Brown EN, Massaquoi SG. Modeling the contribution of lamina 5 neuronal and network dynamics to low frequency EEG phenomena. *Biol Cybern* 2006; 95: 289–310.
- Keihaninejad S, Heckemann RA, Fagiolo G, Symms MR, Hajnal JV, Hammers A. A robust method to estimate the intracranial volume across MRI field strengths (1.5T and 3T.). *Neuroimage* 2010; 50: 1427–37.
- Lempel A, Ziv J. On the complexity of finite sequences. *IEEE Trans Inform Theory* 1976; 22: 75–81.
- Lewis AS, Chetkovich DM. HCN channels in behavior and neurological disease: too hyper or not active enough? *Mol Cell Neurosci* 2011; 46: 357–67.
- Lison H, Happel MF, Schneider F, Baldauf K, Kerbstat S, Seelbinder B, et al. Disrupted cross-laminar cortical processing in beta amyloid pathology precedes cell death. *Neurobiol Dis* 2014; 63: 62–73.
- Nakamura A, Cuesta P, Fernandez A, Arahata Y, Iwata K, Kuratsubo I, et al. Electromagnetic signatures of the preclinical and prodromal stages of Alzheimer's disease. *Brain* 2018; 141: 1470–85.
- Ni Mhuirheartaigh R, Warnaby C, Rogers R, Jbabdi S, Tracey I. Slow-wave activity saturation and thalamocortical isolation during propofol anesthesia in humans. *Sci Transl Med* 2013; 5: 208ra148.
- Olsson A, Vanderstichele H, Andreassen N, De Meyer G, Wallin A, Holmberg B, et al. Simultaneous measurement of beta-amyloid(1-42), total tau, and phosphorylated tau (Thr181) in cerebrospinal fluid by the xMAP technology. *Clin Chem* 2005; 51: 336–45.
- Palop JJ, Mucke L. Network abnormalities and interneuron dysfunction in Alzheimer disease. *Nat Rev Neurosci* 2016; 17: 777–92.
- Passero S, Rocchi R, Vatti G, Burgalassi L, Battistini N. Quantitative EEG mapping, regional cerebral blood flow, and neuropsychological function in Alzheimer's disease. *Dementia* 1995; 6: 148–56.
- Porjesz B, Almasy L, Edenberg HJ, Wang K, Chorlian DB, Foroud T, et al. Linkage disequilibrium between the beta frequency of the human EEG and a GABAA receptor gene locus. *Proc Natl Acad Sci USA* 2002; 99: 3729–33.
- Rasmussen MK, Mestre H, Nedergaard M. The glymphatic pathway in neurological disorders. *Lancet Neurol* 2018; 17: 1016–24.
- Rosengren LE, Karlsson J-E, Karlsson J-O, Persson LI, Wikkelso C. Patients with amyotrophic lateral sclerosis and other neurodegenerative diseases have increased levels of neurofilament protein in CSF. *J Neurochem* 1996; 67: 2013–8.
- Saito Y, Inoue T, Zhu G, Kimura N, Okada M, Nishimura M, et al. Hyperpolarization-activated cyclic nucleotide gated channels: a potential molecular link between epileptic seizures and Abeta generation in Alzheimer's disease. *Mol Neurodegener* 2012; 7: 50.
- Schartner M, Seth A, Noirhomme Q, Boly M, Bruno MA, Laureys S, et al. Complexity of multi-dimensional spontaneous EEG decreases during propofol induced general anaesthesia. *PLoS One* 2015; 10: e0133532.